4716 J. Med. Chem. 2009, 52, 4716–4724
DOI: 10.1021/jm900159g

Journal of Medicinal Chemistry Article

Small Molecule Chloropyramine Hydrochloride (C4) Targets the Binding Site of Focal Adhesion Kinase and Vascular Endothelial Growth Factor Receptor 3 and Suppresses Breast Cancer Growth in Vivo

Elena V. Kurenova,[†] Darell L. Hunt,[‡] Dihua He,[‡] Andrew T. Magis,[§] David A. Ostrov,[§] and William G. Cance*,[†]

[†]*Department of Surgical Oncology, Roswell Park Cancer Institute, Buffalo, New York 14263,* [‡]*Department of Surgery and* [§]*Department of Pathology, Immunology and Laboratory Medicine, University of Florida, College of Medicine, Gainesville, Florida 32610*

Received February 6, 2009

FAK is a tyrosine kinase that functions as a key orchestrator of signals leading to invasion and metastasis. Since FAK interacts directly with a number of critical proteins involved in survival signaling in tumor cells, we hypothesized that targeting a key protein−protein interface with druglike small molecules was a feasible strategy for inhibiting tumor growth. In this study, we targeted the protein−protein interface between FAK and VEGFR-3 and identified compound C4 (chloropyramine hydrochloride) as a drug capable of (1) inhibiting the biochemical function of VEGFR-3 and FAK, (2) inhibiting proliferation of a diverse set of cancer cell types in vitro, and (3) reducing tumor growth in vivo. Chloropyramine hydrochloride reduced tumor growth as a single agent, while concomitant administration with doxorubicin had a pronounced synergistic effect. Our data demonstrate that the FAK−VEGFR-3 interaction can be targeted by small druglike molecules and this interaction can provide the basis for highly specific novel cancer therapeutics.

Introduction

Tumor cell survival requires that tumor cells acquire the ability to survive the apoptotic stimuli associated with invasion and metastasis. Focal adhesion kinase (FAK[a]) and vascular endothelial growth factor receptor 3 (VEGFR-3) are tyrosine kinases that have been identified as critical signaling molecules for these host−tumor interactions.[1,2] FAK is a protein tyrosine kinase that is localized at contact points between cells and extracellular matrix (ECM) and is a point of convergence of a number of signaling pathways associated with cell adhesion, invasion, motility, and angiogenesis.[3−5] This signaling requires both FAK kinase activity and its ability to form multiple protein complexes.[6−10] Targeting of FAK by anti-FAK antibody,[11,12] FAK dominant negative FAK-CD,[9,13] antisense oligonucleotides,[14] or siRNA[15−17] results in cell rounding, detachment, and apoptosis. FAK is emerging as an attractive target for the treatment of cancer because it has been shown that FAK is up-regulated in a broad range of solid tumors and is expressed at very low levels in normal tissues, creating an optimal setting for FAK-targeted cancer therapeutics.[18,19] Indeed, control of FAK signaling has been suggested as a potential anticancer therapy[20,21] and several FAK kinase inhibitors recently have been developed.[22−24]

VEGFR-3 or Flt4 is a receptor tyrosine kinase playing a major role in lymphangiogenesis, angiogenesis and has also been linked to tumorigenesis.[2,25] VEGFR-3 is activated by its specific ligands, VEGF-C and VEGF-D, which promote cancer progression.[26] The VEGF-C/VEGFR-3 axis is expressed in a variety of human tumor cells, and its activation has been shown to promote metastasis.[27] Importantly, it has been shown that inhibition of VEGFR-3 signaling leads to both regression of the lymphatic network and suppression of tumor lymph node metastasis.[28] VEGFR-3 is up-regulated in the microvasculature of tumors and wounds,[29,30] and recently, blocking VEGFR-3 has been shown to suppress angiogenic sprouting in tumors.[2] While there is some controversy regarding the levels of expression of VEGFR-3 in tumor cells,[31,32] VEGFR-3 remains an attractive target for cancer therapy.

Previously we have shown that VEGFR-3 and FAK physically interact in cancer cells, and this provides a survival advantage for the tumor cells.[7] Thus, we have sought to develop novel molecular therapeutics by targeting the VEGFR-3−FAK site of interaction and disrupting their survival function. In the current study we utilized the crystal structure of the FAK focal adhesion targeting (FAT) domain for molecular docking of small molecules that target the VEGFR-3 binding site on FAK. We identified a small molecule compound C4[33](chloropyramine hydrochloride, a histamine receptor H1 antagonist, **1**) that disrupted VEGFR-3−FAK binding and abrogated the phosphorylation of VEGFR-3 while reducing the phosphorylation of FAK. In vitro testing of this compound resulted in the selective growth inhibition and induction of apoptosis in many cancer cell lines, especially those that overexpressed VEGFR-3. In vivo, **1** showed a marked reduction of tumor growth and was synergistic with doxorubicin chemotherapy in breast cancer xenograft models. These results have demonstrated that targeting the FAK−VEGFR-3 interaction with a small molecule compound can disrupt the survival function of these two tyrosine kinases, representing a unique approach for molecular-targeted cancer therapeutics.

*To whom correspondence should be addressed. Phone: 716-845-8204. Fax: 716-845-3434. E-mail: William.Cance@roswellpark.org.

[a] Abbreviations: FAK, focal adhesion kinase; FAT, focal adhesion targeting domain; VEGFR-3, vascular endothelial growth factor receptor 3; ECM, extracellular matrix; MTS, 3-(4,5-dimethylthiazol-2-yl)-5-(3-carboxymethoxyphenyl)-2-(4-sulfophenyl)-2*H*-tetrazolium.

 Published on Web 07/17/2009

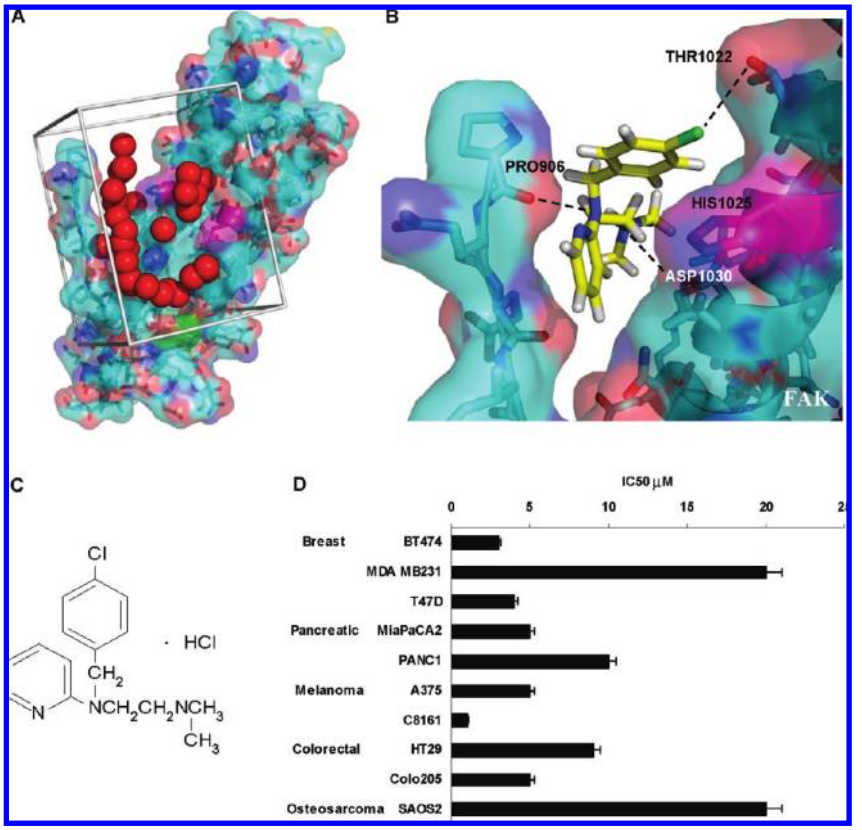

Figure 1. Structure-based development of small molecules that targeted the binding of FAK and VEGFR-3. (A) Site selection for high throughout virtual screening of druglike compounds to develop small molecule FAK inhibitors. The crystal structure of the focal adhesion targeting (FAT) domain of FAK was obtained from the Protein Data Bank (PDB code 1K04) and prepared for computational docking. The 140 000 small molecules from the NCI's Development Therapeutics Program were each positioned in the structural pocket and scored for electrostatic and van der Waals interactions as implemented in DOCKv5.2 package9 (UCSF). The crystal structure is shown in cyan and salmon, and residues that undergo shifts upon peptide binding in NMR studies are shown in magenta. The catalytic tyrosine is shown in green. Red spheres indicate the site defined by the program SPHGEN (UCSF) with chemical and geometric features appropriate for specific small molecule binding. Gray bars demarcate the scoring grid utilized to calculate interactions between potential ligands and the targeted structural pocket. (B) Predicted binding site of **1** to focal adhesion targeting domain of FAK. Histidine 1025 shown in magenta with surrounding residues. Black dashed lines indicate hydrogen bonds between proline 906 and **1** N2, aspartic acid 1030 hydroxyl group and **1** N1, and also hydroxyl group of threonin1022 and Cl of **1**. (C) Compound **1** (chlorpyramin hydrochloride) structure. (D) **1** treatment decreased the viability of a diverse set of cancer cell types. MTS assay was performed on selected cell lines. Cells were treated with the increased concentration of **1** for 72 h and analyzed with Cell Titer Proliferation Assay. Error bars represent ± SEM, $P < 0.05$.

Results

Structure-Based Development of Small Molecules That Targeted the Binding of FAK and VEGFR-3. We previously demonstrated binding of the 12 amino acid peptide of VEGFR-3 to the C-terminal, focal adhesion targeting (FAT) domain of FAK.[7] Nuclear magnetic resonance analysis (NMR) of the FAT/VEGFR-3 peptide complex localized chemical shift of residue histidine 1025 on the FAT domain (Prutzman and Campbell, unpublished data), so we hypothesized that a small molecule binding to this site could disrupt the FAK−VEGFR-3 interaction. Therefore, we used the crystal structure of the FAT domain of FAK[34] to dock small molecules from the NCI/DTP database to the binding region in silico (Figure 1A,B). We selected compounds with the highest binding affinities to FAK for functional testing and selected compound **1** (Figure 1B, C) for its profound inhibitory effect on cell growth. Figure 1B illustrates the binding mode of **1** with the FAK FAT domain. In a panel of breast, colon, lung, osteosarcoma, melanoma, and pancreas cancer cells, the IC_{50} of **1** varied between 1 and 20 μM (Figure 1D). Because **1** was an orally bioavailable antihistamine that inhibited cell survival, we selected it for further mechanistic analyses, focusing on human breast cancer.

1 specifically decreased the viability and proliferation and caused apoptosis in breast cancer cells that expressed VEGFR-3. To further characterize small molecule **1** and its specificity, we used two model systems of breast cancer: BT474 breast cancer cells with high endogenous expression of VEGFR-3 that we previously used to assess the FAK−VEGFR-3 interaction[7] and MCF7 breast cancer cells with undetectable endogenous VEGFR-3 expression that were engineered to overexpress VEGFR-3 (Supporting Information Figure S1). Cells were treated with increasing concentrations of **1**, and viability was measured with MTS assay. BT474 cells were highly sensitive to **1** treatment, whereby 1 μM concentration caused a 40% reduction of viability after 48 h of treatment (Figure 2A). In addition, we found that the effect of **1** was more pronounced in the BT474 breast cancer cells compared to MCF10A "normal" breast epithelial cells (Supporting Information Figure S2A). Next, we tested the specificity of small molecule **1** in the MCF7−VEGFR-3 overexpressing cells. We found that at 1 μM concentration of **1**, viability of control MCF7−pcDNA3 cells was significantly higher than the viability of MCF7−VEGFR-3 cells (Figure 2A,

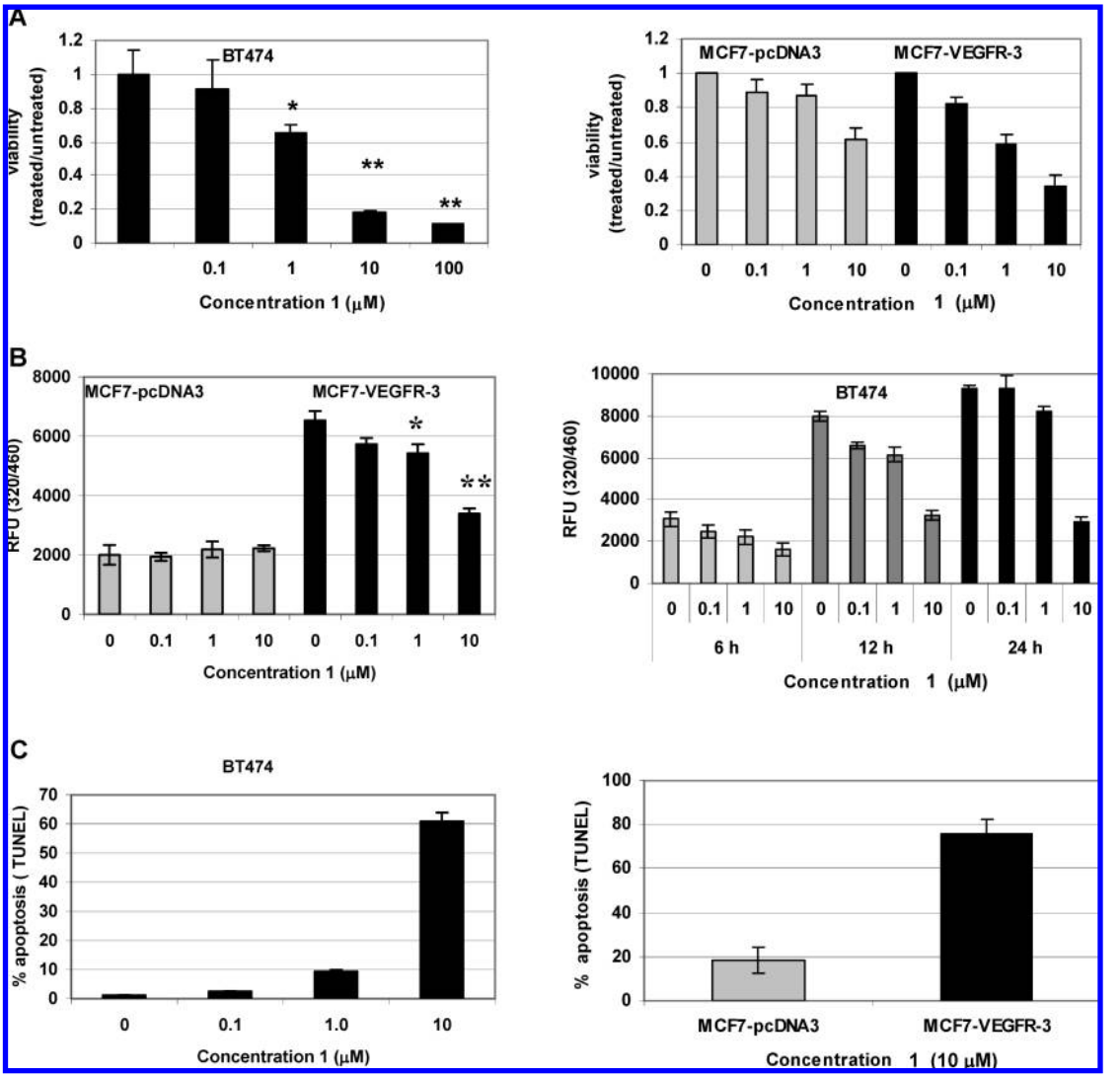

Figure 2. **1** specifically decreased the viability and proliferation and caused apoptosis in breast cancer cells that expressed VEGFR-3. BT474 breast cancer cells with endogenous high VEGFR-3 expression and stable clones of MCF7 breast cancer cells with undetectable VEGFR-3 expression, transfected with either control vector pcDNA3 or VEGFR-3, were treated with the marked concentration of **1**. (A) **1** caused a dose-dependent cytotoxicity of VEGFR-3 expressing cells. The viability was measured in MTS assays after 48 h of treatment: (*) $P < 0.01$; (**) $P < 0.001$. (B) **1** caused a dose-dependent and a time-dependent decrease in proliferation of VEGFR-3 expressing cells: BrdU incorporation assay, (*) $P < 0.05$, (**) $P < 0.001$. (C) **1** treatment caused dose-dependent apoptosis, and proapoptotic effect of **1** is specific for cells expressing VEGFR3: TUNEL assay.

$P < 0.01$) and at 10 μM concentration this difference reached 2-fold (Figure 2A, $P < 0.001$). This demonstrated that cells expressing low levels of VEGFR-3 were less sensitive to **1** inhibition than those that overexpressed this protein. Taken together, these data suggested that **1** specifically inhibited the viability of cells overexpressing VEGFR-3.

Proliferation assays have shown similar results. MCF7−pcDNA control cells did not show any decrease in proliferation even after 48 h of treatment with 10 μM **1** (Figure 2B, gray bars). In contrast, MCF7−VEGFR-3 cells not only proliferated much more quickly than vector controls but were also sensitive to **1** treatment. In these VEGFR-3-overexpressing cells, a similar concentration of **1** for 48 h reduced proliferation approximately 50%, demonstrating that the antiproliferative effect of **1** is VEGFR-3 specific (Figure 2B). We also confirmed that proliferation of normal MCF10A cells was not affected by small molecule **1** (Supporting Information Figure S2B). Similarly, in the BT474 cells, treatment with **1** also led to a concentration-dependent decrease of cell proliferation (Figure 2B). We also found that there was no significant increase in BrdU incorporation in these cells exposed to 10 μM **1** for more than 12 h. We concluded that 10 μM **1** had a cytostatic effect on BT474 cells that might lead to apoptosis at later time points.

When treatment with **1** was continued for 48 h, the breast cancer cells that overexpressed VEGFR-3 underwent apoptosis. This effect was dose-dependent, with 10 μM **1** inducing apoptosis in more than 60% of BT474 cells (Figure 2C). Furthermore, we found that apoptosis caused by **1** was related to the level of VEGFR-3 expression. In our model cell lines MCF7−pcDNA3 and MCF7−VEGFR-3, treatment with 10 μM **1** for 48 h led to a 4-fold increase in apoptotic cell death in the cell line that overexpressed VEGFR-3 (18% versus 76%, respectively) (Figure 2C). We confirmed these results biochemically by measuring the cleavage of PARP and the activation of caspase 8 (Supporting Information Figure S3). From these experiments, we concluded that **1** caused VEGFR-3-dependent apoptosis in breast cancer cells.

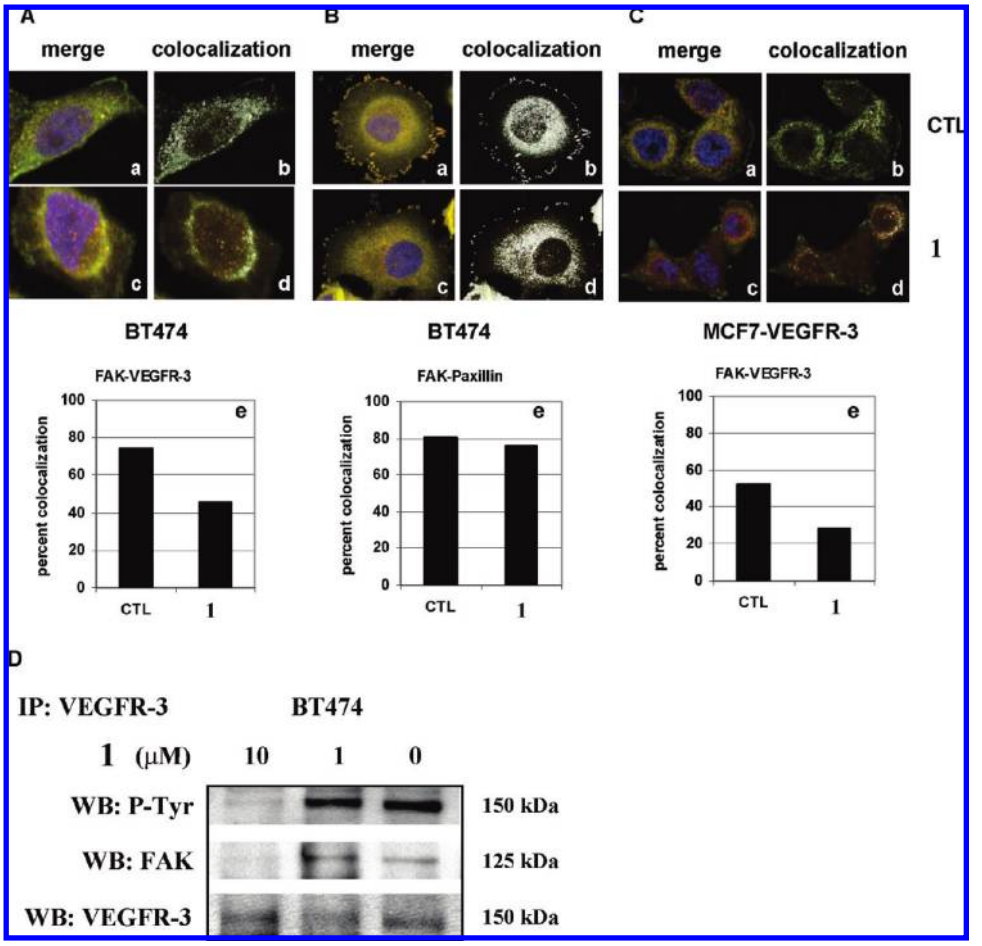

Figure 3. **1** treatment affected colocalization and led to redistribution and decrease of FAK−VEGFR-3 complexes. Cells were treated with DMSO (CTL, all panels a and b) or 10 μM **1** (all panels c and d) for 24 h, immunostained for FAK (green, Alexa Fluor 488) in combination with VEGFR-3 or paxillin (red, Alexa Fluor 546). Colocalization in treated and untreated cells was assessed by confocal microscopy and scatter plot analysis (e). (A) Treatment with small molecule **1** caused decrease in colocalization of FAK and VEGFR-3 in BT474 cells: (a) merged image, control cells; (b) colocalization, control cells; (c) merged image, **1** treated cells; (d) colocalization, **1** treated cells; (e) percentage of colocalized FAK and VEGFR-3 molecules in control and **1** treated cells. (B) FAK−paxillin complexes were not affected by treatment with small molecule **1**. (a−e) Percentage of colocalized FAK and paxillin molecules in control and **1** treated BT474 cells. (C) **1** caused decrease in colocalization of VEGFR-3 and FAK in MCF7 cells that overexpressed VEGFR-3. (a−e) Percentage of colocalized FAK and VEGFR-3 molecules in control and **1** treated MCF7−VEGFR-3 cells. (D) **1** disrupted binding of the FAK and VEGFR-3 proteins. Immunoprecipitation with VEGFR-3 antibody after treatment for 24 h with increasing concentrations of compound **1** revealed a decreased amount of FAK protein coprecipitated with VEGFR-3.

1 disrupted the FAK−VEGFR-3 complex. To determine the effects of **1** on the interaction of FAK and VEGFR-3, we analyzed the distribution of FAK and VEGFR-3 in the BT474 and MCF7−VEGFR-3 cells after treatment. As a control, we also tested a different focal adhesion protein, paxillin that bound to the FAT domain close to the VEGFR-3 binding site. Cells were dually immunostained for FAK in combination with either VEGFR-3 or paxillin, and confocal microscopy was used to calculate the degree of colocalization by scatter plot analysis. In untreated cells, stained for FAK and paxillin, we found that approximately 80% of the FAK and paxillin molecules were colocalized in BT474 cells and positioned predominantly in focal adhesions (Figure 3B, panels a, b, e). Similarly, the colocalization of VEGFR-3 with FAK was also high in untreated cells, with a rate of 80% for BT474 (Figure 3A, panels a, b, e) and 50% for MCF7−VEGFR-3 cells (Figure 3C, panels a, b, e), and occurring predominantly in the cytoplasm, as we have shown previously.[7] When BT474 cells were treated with **1**, the FAK−paxillin localization was not affected (80% nontreated vs 76% treated, Figure 3B, panels c, d, e). In contrast, **1** treatment dramatically decreased the colocalization of FAK and VEGFR-3 in the cytoplasm of both BT474 and MCF7−VEGFR-3 cells, reducing it to 45% and 29% respectively (Figure 3A and 3C, panels c, d, e). This drop in colocalized FAK and VEGFR-3 molecules correlated with intracellular redistribution of these proteins after **1** treatment, revealed by confocal microscopy and 3D reconstruction of the confocal images. **1** treatment led to redistribution of FAK and VEGFR-3 inside the cells but did not affect the localization of paxillin (Supporting Information Figure S4). We confirmed this effect on multiple samples of BT474 and MCF7−VEGFR-3 cells and with different FAK and VEGFR-3 antibody (Supporting Information Figure S5A,B).

Next, we used immunoprecipitation to confirm that **1** disrupted FAK and VEGFR-3 binding. BT474 cells were treated with an increasing concentration of **1**, and the proteins were coprecipitated with VEGFR-3 antibody. We found that treatment with 10 μM **1** for 24 h dramatically decreased the amount of FAK−VEGFR-3 associated molecules

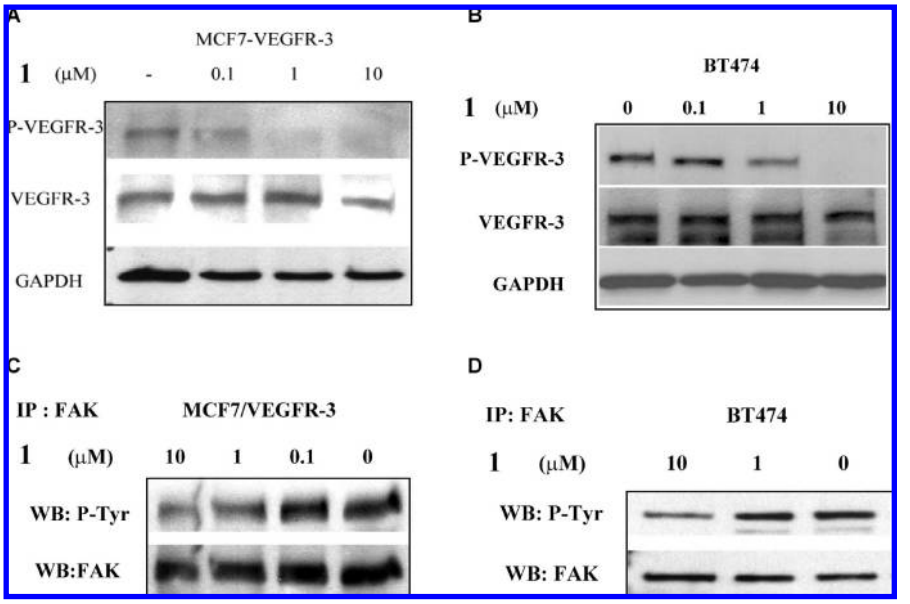

Figure 4. **1** treatment caused dose-dependent dephosphorylation of VEGFR-3 and decreased phosphorylation of FAK. (A, B) Western blot analysis of MCF7−VEGFR-3 breast cancer cells and BT474 breast cancer cells after 24 h of treatment with increasing doses of **1**. VEGFR-3 phosphorylation was analyzed. (C, D) Immunoprecipitation of FAK and Western blot analysis with antiphosphotyrosine antibody 4G10 of MCF7−VEGFR-3 and BT474 cells treated for 24 h with 10 μM or 1 μM **1**.

(Figure 3D). Thus, small molecule **1** specifically targeted the FAK−VEGFR-3 interaction and disrupted the binding of these proteins in the breast cancer cells.

1 caused dose-dependent dephosphorylation of both VEGFR-3 and FAK. To further characterize the biochemical effects of **1** on VEGFR-3 and FAK, we treated cells with different concentrations of **1** and analyzed for the phosphorylation of Tyr1063/1068 in the activation loop of the VEGFR-3 kinase domain. We found that a 24 h treatment with 1 μM **1** caused a partial dephosphorylation of this site and 10 μM completely dephosphorylated this activation site of VEGFR-3 (Figure 4A,B). This effect was dose and time dependent and appeared to be specific for VEGFR-3 because it did not affect phosphorylation of other tyrosine kinases including Src, EGFR, PDGFR, and IGF-1R (data not shown). At the same time this effect was **1**-specific, as other small molecules, selected for the FAK−VEGFR-3 binding site, did not affect VEGFR-3 phosphorylation (Supporting Information Figure S3C). Next, we assessed changes in the total phosphorylation of FAK. We found that 10 μM **1** treatment for 24 h decreased total FAK phosphorylation in both model cell lines (Figure 4C,D). Taken together, these results show that **1** reduces the phosphorylation of both VEGFR-3 and FAK. Since dephosphorylation of FAK has been shown to result in disruption of FAK from its position in the focal adhesions and lead to apoptosis,[14] these biochemical results are consistent with our findings that **1** treatment caused apoptosis in the tumor cells.

1 decreased tumor growth in vivo and sensitized the tumors to chemotherapy. To further validate the activity of small molecule **1**, we employed a tumor xenograft mouse model. Female nude mice were subcutaneously inoculated with either the BT474 breast cancer cells or the MCF7 breast cancer cells that stably overexpressed VEGFR-3. Treatment with small molecule **1** (60 mg/kg) was started the day after injection of the cells and given for a total of 21 days. **1** caused a dramatic reduction of tumor growth in both model systems whereby the tumor size in the treated groups was approximately 20% of the tumor size in vehicle control groups (Figure 5, Supporting Information Figure S6A,B). Similarly, the weights of the tumors in the treated group were approximately 4 times less than in the untreated groups (Supporting Information Figure S6C). These results demonstrated significant in vivo efficacy of **1**.

We also compared **1** with a different histamine receptor H1 antagonist **2** (diphenhydramine) and found that it did not have any effect on tumor growth when **1** reduced tumor growth more than 75% (Figure 6A). Thus, we concluded that the antitumor efficacy of **1** is not related to its antihistamine properties.

Next, we tested the efficacy of the combination of **1** with standard chemotherapy for breast cancer, because our in vitro experiments have shown that **1** sensitized breast cancer cells to doxorubicin treatment (data not shown). We tested this combination approach in vivo by concomitant administration of lower dose **1** (10 mg/kg daily) and low-dose of doxorubicin (0.3 mg/kg/week) in mice bearing BT474 xenografts. Doxorubicin administered at 3 mg/kg caused approximately 60% reduction of tumor growth but had no effect on tumor growth at 0.3 mg/kg (Figure 6B, triangles). In contrast, there was a modest effect of **1** alone (50% reduction of tumor growth, Figure 6B, rectangles). However, the low-dose combination of **1** and doxorubicin had a prolonged antitumor effect (85% reduction of tumor growth) that was greater than either drug alone (Figure 6B, dots). These data demonstrated a synergistic effect of the combination of **1** with standard chemotherapy for breast cancer.

Discussion

In this report, we have demonstrated a unique approach to cancer treatment by inhibiting FAK and VEGFR-3 through targeting the site of their protein−protein interaction. This study has demonstrated that we can inhibit the function of these tyrosine kinases by targeting their binding site. Moreover, our computational approach for molecular docking has

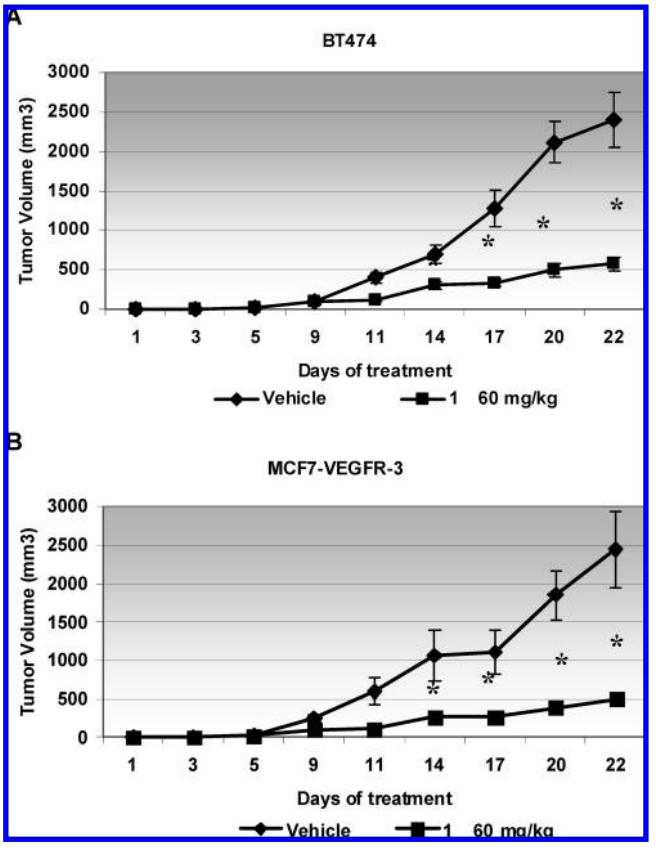

Figure 5. **1** reduced tumor growth in mouse xenograft models. BT474 (A) or MCF7−VEGFR-3 (B) cells were inoculated into mice subcutaneously. Treatment with 60 mg/kg **1** or vehicle (PBS) was started the day after cell inoculation. Mice were sacrificed 21 days later, and tumors were measured for size and weight (Supporting Information Figure S6). BT474 and MCF7−VEGFR-3 **1**-treated tumor volumes were significantly smaller than vehicle treated tumors after day 14: (∗) $P < 0.01$.

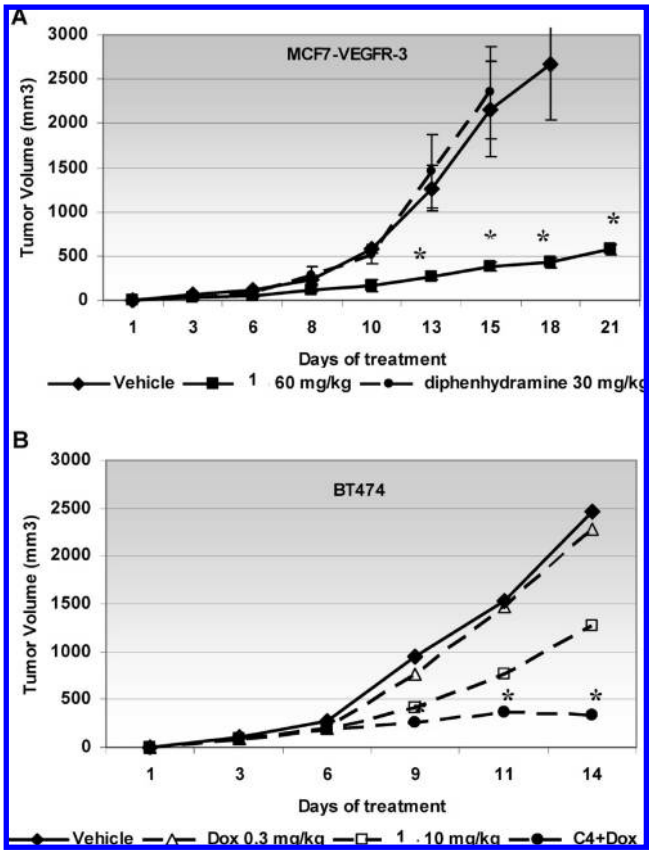

Figure 6. The **1** antitumor effect is not related to its antihistamine properties, and it sensitizes tumors to chemotherapy treatment with doxorubicin at low concentration. (A) MCF7−VEGFR-3 cells were inoculated into mice subcutaneously. Treatment with 60 mg/kg **1**, 30 mg/kg **2** (diphenhydramine), or vehicle (PBS) daily was started the next day. (B) BT474 cells were inoculated into mice subcutaneously. Treatment with 10 mg/kg **1** daily or doxorubicin 0.3 mg/kg weekly or the combination of both drugs was started the next day after cell inoculation. Experiments were terminated after 14 days when tumor size of single treatment reached protocol end point. Statistically significant difference (∗, $P < 0.01$) with vehicle treated tumors was seen from day 9.

identified a small molecule that not only decreased activity of both VEGFR-3 and FAK but had antitumor effects that were synergistic with chemotherapy in vivo.

We selected the VEGFR-3 binding site on the FAT domain of FAK as a template for our in silico studies because of the importance of both of these kinases in cancer cell survival and tumor progression. We virtually docked potential small molecules and identified compound **1** (chloropyramine hydrochloride). It was functionally equivalent to the FAK-inhibiting peptide from the VEGFR-3,[7] decreased cell proliferation, and caused apoptosis in breast cancer cells. To prove that this small molecule affects interaction of VEGFR-3 with FAK, we analyzed FAK−VEGFR-3 colocalization and coprecipitation in immunohistochemical and biochemical experiments. We have shown that treatment with **1** decreased colocalization and FAK−VEGFR-3 complex formation. Thus, in silico modeling demonstrated that peptide binding sites of FAK are appropriate targets for non-peptide small druglike molecule binding.

Studies with peptide inhibitors already have indicated that blockade of specific protein−protein interactions have therapeutic promise for treating a variety of human cancers.[35−37] The major advantage of protein−protein inhibitors is their high selectivity. For example, the nutlins inhibitors of the p53-MDM2 interaction activated apoptosis in cells expressing wild-type p53 and showed a 10- to 20-fold selectivity for cells with active versus mutated p53.[38] In the present study, targeting the site of FAK−VEGFR-3 protein−protein interaction represents a novel approach to targeting tyrosine kinases that can potentially be used to disrupt their "interactome" and inhibit specific downstream signaling. Until now, the main approach to target FAK was to inhibit the catalytic activity of the tyrosine kinase by interfering with the binding of ATP. Three such inhibitors have been reported by Novartis[22] and Pfizer.[23,24] All of them inhibit FAK kinase activity but have varying degrees of cross-reactivity with other tyrosine kinases.[39] Similarly, the only known inhibitor for VEGFR-3 is MAZ-51, which suppressed mammary tumor growth in rats,[40] but not having a broad clinical utility. Clinically, broad range tyrosine kinase inhibitors are being used to target the VEGFR family in addition to other receptor tyrosine kinases with varying degrees of success.[41] In this study, we have shown the specificity of **1** for FAK and VEGFR-3 whereby it changed the phosphorylation and activation status of VEGFR-3 and FAK by disrupting their interaction and did not have a demonstrable effect on the activity of other receptor and nonreceptor protein kinases.

The small molecule **1** that targeted the FAK−VEGFR-3 binding site was chloropyramine hydrochloride, belonging to

the class of antagonists of histamine receptor H1. This small molecule was analyzed in mouse ascites tumor experiments of Honti and Puntoky over 40 years ago[42] when the hypothesis that histamine might be involved in carcinogenesis was proposed,[43] but the results were inconclusive. In our experiments, we have shown a unique biological specificity of this drug for the FAK−VEGFR-3 interaction. In our breast cancer xenograft models, we have shown that treatment with **1** reduced tumor burden more than 80%, and this effect was not related to its antihistamine properties when compared to the histamine blocker **2**.

One of the most significant aspects of our findings relates to the ability of **1** to sensitize breast cancer cells to chemotherapy. When **1** was administered with the standard chemotherapeutic for breast cancer, doxorubicin, we saw a pronounced synergistic effect, and this effect was still significant when we reduced the dose of both drugs. Because FAK is a survival signal and has been directly implicated in chemoresistance,[44] we hypothesize that the decreased phosphorylation of FAK and VEGFR-3 caused by **1** results in a greater sensitivity of the cancer cells to chemotherapy.

In summary, our data suggest that the FAK−VEGFR-3 protein−protein interaction is an excellent site to develop small molecule inhibitors to provide the basis for highly specific novel cancer therapeutic agents. When this interaction is targeted, survival signaling in the tumors can be interrupted, and this may provide a useful method of augmenting the effects of chemotherapy in breast cancer.

Experimental Section

Virtual Screening. The DOCKv5.2 package9 was used for in silico screening of approximately 140 000 compounds available from the National Cancer Institute Developmental Therapeutics Program. This small molecule database was prepared with the DOCK accessory software SF2MOL2 (University of California—San Francisco) and Sybyl (Tripos, Inc.) as described previously.[45] The crystal structure for focal adhesion kinase (PDB code 1K04[34]) was obtained from the Protein Data Bank. All heteroatoms and water molecules were removed, and a single chain was isolated in the coordinate file. The program DMS was used to generate a molecular surface.[46] SPHGEN was used to generate spheres on the surface of the protein, and a subset of these spheres within 5 Å of the target pocket was selected to constrain the search space (Figure 1A). Molecular mechanics force field grids were generated using the program GRID, using the standard 6−12 Lennard-Jones function to approximate the van der Waals forces. Finally, DOCK 5.2 was executed using the prepared files and the small molecule database. Each compound was docked as a rigid body in up to 100 different orientations. The orientations were filtered by default bump filter parameters to exclude compounds with pronounced steric clashes. The top compounds predicted to interact with the target site were subsequently obtained from the National Cancer Institute.

Cell Lines. MCF7, MDA-MB-231, T47D, A549, SAOS-2, A375, C8161, PANC1, MiaPaCa-2, HT29, and Colo205 cells were purchased from ATCC (Rockville, MD). The BT474 cells are a subclone of the original cell line that does not express the receptor tyrosine kinase Her-2/neu. BT474 cells were maintained in RPMI-1640 with 10% fetal bovine serum and insulin, 250 μg/mL. MCF7−pcDNA3 and MCF7−VEGFR-3 stable clones of the MCF7 breast cancer cell line were produced as described (Supporting Information Figure S1). All cells are maintained in correspondence with ATCC recommendations.

Antibodies and Reagents. Antihuman VEGFR-3 antibodies were purchased from Chemicon (MAB3757, clone 9D9F9, Temecula, CA) and from Santa Cruz Biotechnology (sc-321), phospho-specific VEGFR-3 antibody (pc460) was from Calbiochem (San Diego, CA), FAK antibody 4.47 was from Upstate and sc-558 from Santa Cruz Biotechnology, phospho-specific Y-397 antibody MAB1144 was from Chemicon, and phosphotyrosine specific antibody 4G10 (no. 05-321) was from Upstate. The following were from Cell Signaling Technology (Danvers, MA): procaspase-8 (no. 9746), Erk 1,2 (no. 9102), p-Erk (no. 4377S), Akt (no. 9272), p-Akt (no. 9271), PARP (no. 9542), and paxillin antibody no. 610051 from BD Biosciences.

Compound **1** was obtained as chlorpyramin hydrochloride (Sigma, no. 1915), solution for injection 20 mg/mL (EGIS, Hungary), 60 μL/injection, 60 mg/kg. Also obtained was diphenhydramine (solution for injections 10 mg/mL), 60 μL/injection, 30 mg/kg. Doxorubicin hydrochloride injection, USP, is a sterile, isotonic solution, 2 mg/mL, and was used as 30 μL/injection, 3 mg/kg, and 10× dilution, 0.2 mg/mL, 30 μL/injection, 0.3 mg/kg. All chemicals were of the highest purity commercially available.

Immunocytochemistry. Cells were incubated in presence or absence of **1** and stained with anti-FAK antibody 4.47 or in combination with paxillin or VEGFR-3 as previously described[7,9] and described in Supporting Information. Detection was done with Alexa Fluor 546 secondary antibody, and for dual staining the combination of Alexa Fluor 488 and Alexa Fluor 546 secondary antibody were used (Invitrogen, Carlsbad, CA). The slides were observed on a Leica confocal microscope (Leica TCS SP5) running Leica LAS-AF software for instrument control and image analysis.

Assays of Cell Viability. Cell survival was assayed in MTS (3-(4,5-dimethylthiazol-2-yl)-5-(3-carboxymethoxyphenyl)-2-(4-sulfophenyl)-2*H*-tetrazolium) assay by measuring mitochondrial dehydrogenase activity of metabolically active cells with Cell Titer 96 AQueous One Solution Cell Proliferation Assay (Promega, Madison, WI). The 5.0×10^3 (100 μL) cells were plated in 96-well plates and were allowed to attach overnight. Then 100 μL of fresh medium with or without **1** was added to each well. Cells were treated for the designated amount of time. MTS assay was performed according to the manufacturer's protocol.

Detection of apoptosis was performed by TUNEL assay with the APO-DIRECT kit (Pharmingen, BD Biosciences, San Diego, CA) according to the manufacturer's recommendations and analyzed by flow cytometry. Quantitative analysis of apoptosis was performed using the FlowJo program (Tree Star, Ashland, OR).

Immunoprecipitation and Western Blot Analysis. Appropriately treated or nontreated cells were allowed to grow until they were 80−85% confluent or until treatment was completed. Cells were lysed and used for Western blot or immunoprecipitation as previously described.[7]

BrdU Incorporation Assay. BrdU incorporation was performed using BrdU Cell Proliferation Assay, HTS (Calbiochem, San Diego, CA). The 2.5×10^3 cells were plated into a 96-well plate and allowed to attach overnight. Then 100 μL of fresh growth medium or growth medium with treatment was added to each well followed by 20 μL of BrdU labeling. Cells were incubated for the appropriate time and treated according to the manufacturer's protocol.

Animal Models. BT474 and MCF7−VEGFR-3 cells at a concentration of $(2-5) \times 10^6$ cells per 200 μL were subcutaneously injected into the right flank of the 5−6 week old hsd: athymic nude-*foxn1nu* mice (Harlan), five in each group, in accordance with the University of Florida IACUC approved protocol. Treatment with compound **1** was started the next day after cell injection via intraperitoneal injection (ip) once a day. Tumor size was measured thrice weekly, and volume was calculated using the formula length × width^2 × 0.5. Animals were sacrificed after 21 days of treatment or when tumor size reached protocol end point. Tumor was excised, measured and preserved for protein and RNA preparation and cytochemistry.

Statistical Analysis. Data are represented as the mean ± SEM of three or more independent experiments. For in vitro and in vivo experiments comparison between groups were made using a two-tailed two-sample Student's *t* test. Differences for which the *P* value was less than 0.05 were considered statistically significant.

Acknowledgment. We thank members of the Flow Cytometry Core Laboratory at the Interdisciplinary Center for Biotechnology Research, University of Florida, and especially Steve McClellan, for technical assistance with confocal microscopy and FACS analysis. The Leica TCS SP5 was obtained through a shared instrument grant from the State of Florida Bankhead-Cooley Cancer Research fund. This work was supported by National Cancer Institute Grant CA-65910 (W.G.C.) and Ruth L. Kirschtein National Research Service Award 5 T32 CA106493-02 (D.L.H.).

Supporting Information Available: Experimental procedures and additional biochemical evaluation of compound **1** effect in vitro and in vivo. This material is available free of charge via the Internet at http://pubs.acs.org.

References

(1) Chatzizacharias, N. A.; Kouraklis, G. P.; Theocharis, S. E. Focal adhesion kinase: a promising target for anticancer therapy. *Expert Opin. Ther. Targets* **2007**, *11*, 1315–1328.
(2) Tammela, T.; Zarkada, G.; Wallgard, E.; Murtomaki, A.; Suchting, S.; Wirzenius, M.; Waltari, M.; Hellstrom, M.; Schomber, T.; Peltonen, R.; Freitas, C.; Duarte, A.; Isoniemi, H.; Laakkonen, P.; Christofori, G.; Yla-Herttuala, S.; Shibuya, M.; Pytowski, B.; Eichmann, A.; Betsholtz, C.; Alitalo, K. Blocking VEGFR-3 suppresses angiogenic sprouting and vascular network formation. *Nature* **2008**, *454*, 656–660.
(3) Cox, B. D.; Natarajan, M.; Stettner, M. R.; Gladson, C. L. New concepts regarding focal adhesion kinase promotion of cell migration and proliferation. *J. Cell. Biochem.* **2006**, *99*, 35–52.
(4) Frisch, S. M.; Vuori, K.; Ruoslahti, E.; Chan-Hui, P. Y. Control of adhesion-dependent cell survival by focal adhesion kinase. *J. Cell Biol.* **1996**, *134*, 793–799.
(5) Schlaepfer, D. D.; Mitra, S. K.; Ilic, D. Control of motile and invasive cell phenotypes by focal adhesion kinase. *Biochim. Biophys. Acta* **2004**, *1692*, 77–102.
(6) Chen, R.; Kim, O.; Li, M.; Xiong, X.; Guan, J. L.; Kung, H. J.; Chen, H.; Shimizu, Y.; Qiu, Y. Regulation of the PH-domain-containing tyrosine kinase Etk by focal adhesion kinase through the FERM domain. *Nat. Cell Biol.* **2001**, *3*, 439–444.
(7) Garces, C. A.; Kurenova, E. V.; Golubovskaya, V. M.; Cance, W. G. Vascular endothelial growth factor receptor-3 and focal adhesion kinase bind and suppress apoptosis in breast cancer cells. *Cancer Res.* **2006**, *66*, 1446–1454.
(8) Mamali, I.; Kapodistria, K.; Lampropoulou, M.; Marmaras, V. J. Elk-1 is a novel protein-binding partner for FAK, regulating phagocytosis in medfly hemocytes. *J. Cell. Biochem.* **2008**, *103*, 1895–1911.
(9) Kurenova, E.; Xu, L.-H.; Yang, X.; Baldwin, A. S., Jr.; Craven, R. J.; Hanks, S. K.; Liu, Z.-g.; Cance, W. G. Focal adhesion kinase suppresses apoptosis by binding to the death domain of receptor-interacting protein. *Mol. Cell. Biol.* **2004**, *24*, 4361–4371.
(10) Golubovskaya, V. M.; Cance, W. G. Focal adhesion kinase and p53 signaling in cancer cells. *Int. Rev. Cytol.* **2007**, *263*, 103–153.
(11) Hungerford, J. E.; Compton, M. T.; Matter, M. L.; Hoffstrom, B. G.; Otey, C. A. Inhibition of pp125FAK in cultured fibroblasts results in apoptosis. *J. Cell Biol.* **1996**, *135*, 1383–1390.
(12) Liu, X. J.; Yang, L.; Wu, H. B.; Qiang, O.; Huang, M. H.; Wang, Y. P. Apoptosis of rat hepatic stellate cells induced by anti-focal adhesion kinase antibody. *World J. Gastroenterol.* **2002**, *8*, 734–738.
(13) Heidkamp, M. C.; Bayer, A. L.; Kalina, J. A.; Eble, D. M.; Samarel, A. M. GFP-FRNK disrupts focal adhesions and induces anoikis in neonatal rat ventricular myocytes. *Circ. Res.* **2002**, *90*, 1282–1289.
(14) Xu, L. H.; Owens, L. V.; Sturge, G. C.; Yang, X.; Liu, E. T.; Craven, R. J.; Cance, W. G. Attenuation of the expression of the focal adhesion kinase induces apoptosis in tumor cells. *Cell Growth Differ.* **1996**, *7*, 413–418.
(15) Halder, J.; Kamat, A. A.; Landen, C. N., Jr.; Han, L. Y.; Lutgendorf, S. K.; Lin, Y. G.; Merritt, W. M.; Jennings, N. B.; Chavez-Reyes, A.; Coleman, R. L.; Gershenson, D. M.; Schmandt, R.; Cole, S. W.; Lopez-Berestein, G.; Sood, A. K. Focal adhesion kinase targeting using in vivo short interfering RNA delivery in neutral liposomes for ovarian carcinoma therapy. *Clin. Cancer Res.* **2006**, *12*, 4916–4924.
(16) Jin, Y.-P.; Korin, Y.; Zhang, X.; Jindra, P. T.; Rozengurt, E.; Reed, E. F. RNA interference elucidates the role of focal adhesion kinase in HLA class I-mediated focal adhesion complex formation and proliferation in human endothelial cells. *J. Immunol.* **2007**, *178*, 7911–7922.
(17) Huang, Y. T.; Lee, L. T.; Lee, P. P.; Lin, Y. S.; Lee, M. T. Targeting of focal adhesion kinase by flavonoids and small-interfering RNAs reduces tumor cell migration ability. *Anticancer Res.* **2005**, *25*, 2017–2025.
(18) Cance, W. G.; Harris, J. E.; Iacocca, M. V.; Roche, E.; Yang, X.; Chang, J.; Simkins, S.; Xu, L. Immunohistochemical analyses of focal adhesion kinase expression in benign and malignant human breast and colon tissues: correlation with preinvasive and invasive phenotypes. *Clin. Cancer Res.* **2000**, *6*, 2417–2423.
(19) Carelli, S.; Zadra, G.; Vaira, V.; Falleni, M.; Bottiglieri, L.; Nosotti, M.; Di Giulio, A. M.; Gorio, A.; Bosari, S. Up-regulation of focal adhesion kinase in non-small cell lung cancer. *Lung Cancer* **2006**, *53*, 263–271.
(20) McLean, G. W.; Carragher, N. O.; Avizienyte, E.; Evans, J.; Brunton, V. G.; Frame, M. C. The role of focal-adhesion kinase in cancer—a new therapeutic opportunity. *Nat. Rev. Cancer* **2005**, *5*, 505–515.
(21) van Nimwegen, M. J.; van de Water, B. Focal adhesion kinase: a potential target in cancer therapy. *Biochem. Pharmacol.* **2006**, 597–609.
(22) Shi, Q.; Hjelmeland, A. B.; Keir, S. T.; Song, L.; Wickman, S.; Jackson, D.; Ohmori, O.; Bigner, D. D.; Friedman, H. S.; Rich, J. N. A novel low-molecular weight inhibitor of focal adhesion kinase, TAE226, inhibits glioma growth. *Mol. Carcinog.* **2007**, *46*, 488–496.
(23) Slack-Davis, J. K.; Martin, K. H.; Tilghman, R. W.; Iwanicki, M.; Ung, E. J.; Autry, C.; Luzzio, M. J.; Cooper, B.; Kath, J. C.; Roberts, W. G.; Parsons, J. T. Cellular characterization of a novel focal adhesion kinase inhibitor. *J. Biol. Chem.* **2007**, *282*, 14845–14852.
(24) Roberts, W. G.; Ung, E.; Whalen, P.; Cooper, B.; Hulford, C.; Autry, C.; Richter, D.; Emerson, E.; Lin, J.; Kath, J.; Coleman, K.; Yao, L.; Martinez-Alsina, L.; Lorenzen, M.; Berliner, M.; Luzzio, M.; Patel, N.; Schmitt, E.; LaGreca, S.; Jani, J.; Wessel, M.; Marr, E.; Griffor, M.; Vajdos, F. Antitumor activity and pharmacology of a selective focal adhesion kinase inhibitor, PF-562,271. *Cancer Res.* **2008**, *68*, 1935–1944.
(25) Alitalo, K.; Carmeliet, P. Molecular mechanisms of lymphangiogenesis in health and disease. *Cancer Cell* **2002**, *1*, 219–227.
(26) Skobe, M.; Hawighorst, T.; Jackson, D. G.; Prevo, R.; Janes, L.; Velasco, P.; Riccardi, L.; Alitalo, K.; Claffey, K.; Detmar, M. Induction of tumor lymphangiogenesis by VEGF-C promotes breast cancer metastasis. *Nat. Med.* **2001**, *7*, 192–198.
(27) Su, J.-L.; Yang, P.-C.; Shih, J.-Y.; Yang, C.-Y.; Wei, L.-H.; Hsieh, C.-Y.; Chou, C.-H.; Jeng, Y.-M.; Wang, M.-Y.; Chang, K.-J.; Hung, M.-C.; Kuo, M.-L. The VEGF-C/Flt-4 axis promotes invasion and metastasis of cancer cells. *Cancer Cell* **2006**, *9*, 209–223.
(28) Thiele, W.; Sleeman, J. P. Tumor-induced lymphangiogenesis: a target for cancer therapy?. *J. Biotechnol.* **2006**, *124*, 224–241.
(29) Valtola, R.; Salven, P.; Heikkila, P.; Taipale, J.; Joensuu, H.; Rehn, M.; Pihlajaniemi, T.; Weich, H.; deWaal, R.; Alitalo, K. VEGFR-3 and its ligand VEGF-C are associated with angiogenesis in breast cancer. *Am. J. Pathol.* **1999**, *154*, 1381–1390.
(30) Paavonen, K.; Puolakkainen, P.; Jussila, L.; Jahkola, T.; Alitalo, K. Vascular endothelial growth factor receptor-3 in lymphangiogenesis in wound healing. *Am. J. Pathol.* **2000**, *156*, 1499–1504.
(31) Petrova, T. V.; Bono, P.; Holnthoner, W.; Chesnes, J.; Pytowski, B.; Sihto, H.; Laakkonen, P.; Heikkila, P.; Joensuu, H.; Alitalo, K. VEGFR-3 expression is restricted to blood and lymphatic vessels in solid tumors. *Cancer Cell* **2008**, *13*, 554–556.
(32) Su, J.-L.; Chen, P.-S.; Chien, M.-H.; Chen, P. B.; Chen, Y.-H.; Lai, C.-C.; Hung, M.-C.; Kuo, M.-L. Further evidence for expression and function of the VEGF-C/VEGFR-3 axis in cancer cells. *Cancer Cell* **2008**, *13*, 557–560.
(33) Cance, W. G.; Golubovskaia, V. M.; Kurenova, E. V.; Ostrov, D. A. Focal Adhesion Kinase Protein Binding Inhibitors. Provisional Patent 61/192,192, September 15, **2008**.
(34) Arold, S. T.; Hoellerer, M. K.; Noble, M. E. The structural basis of localization and signaling by the focal adhesion targeting domain. *Structure* **2002**, *10*, 319–327.

(35) Verdine, G. L.; Walensky, L. D. The challenge of drugging undruggable targets in cancer: lessons learned from targeting BCL-2 family members. *Clin. Cancer Res*. **2007**, *13*, 7264–7270.
(36) Arkin, M. Protein−protein interactions and cancer: small molecules going in for the kill. *Curr. Opin. Chem. Biol*. **2005**, *9*, 317–324.
(37) Fry, D. C.; Vassilev, L. T. Targeting protein−protein interactions for cancer therapy. *J. Mol. Med*. **2005**, *83*, 955–963.
(38) Vassilev, L. T.; Vu, B. T.; Graves, B.; Carvajal, D.; Podlaski, F.; Filipovic, Z.; Kong, N.; Kammlott, U.; Lukacs, C.; Klein, C.; Fotouhi, N.; Liu, E. A. In vivo activation of the p53 pathway by small-molecule antagonists of MDM2. *Science* **2004**, *303*, 844–848.
(39) Liu, T.-J.; LaFortune, T.; Honda, T.; Ohmori, O.; Hatakeyama, S.; Meyer, T.; Jackson, D.; de Groot, J.; Yung, W. K. A. Inhibition of both focal adhesion kinase and insulin-like growth factor-I receptor kinase suppresses glioma proliferation in vitro and in vivo. *Mol. Cancer Ther*. **2007**, *6*, 1357–1367.
(40) Kirkin, V.; Thiele, W.; Baumann, P.; Mazitschek, R.; Rohde, K.; Fellbrich, G.; Weich, H.; Waltenberger, J.; Giannis, A.; Sleeman, J. P. MAZ51, an indolinone that inhibits endothelial cell and tumor cell growth in vitro, suppresses tumor growth in vivo. *Int. J. Cancer* **2004**, *112*, 986–993.
(41) Olsson, A.-K.; Dimberg, A.; Kreuger, J.; Claesson-Welsh, L. VEGF receptor signalling—in control of vascular function. *Nat. Rev. Mol. Cell Biol*. **2006**, *7*, 359–371.
(42) Honti, G.; Putnoky, G. The effect of subcutaneously administered suprastin on ascites tumor strains in mice. *Z. Gesamte Inn. Med. Ihre Grenzgeb*. **1963**, *18*, 801–803.
(43) Kahlson, G.; Rosengren, E. New approaches to the physiology of histamine. *Physiol. Rev*. **1968**, *48*, 155–196.
(44) van Nimwegen, M. J.; Huigsloot, M.; Camier, A.; Tijdens, I. B.; van de Water, B. Focal adhesion kinase and protein kinase B cooperate to suppress doxorubicin-induced apoptosis of breast tumor cells. *Mol. Pharmacol*. **2006**, *70*, 1330–1339.
(45) Sandberg, E. M.; Ma, X.; He, K.; Frank, S. J.; Ostrov, D. A.; Sayeski, P. P. Identification of 1,2,3,4,5,6-hexabromocyclohexane as a small molecule inhibitor of jak2 tyrosine kinase autophosphorylation [correction of autophophorylation]. *J. Med. Chem*. **2005**, *48*, 2526–2533.
(46) Richards, F. M. Areas, volumes, packing and protein structure. *Annu. Rev. Biophys. Bioeng*. **1977**, *6*, 151–176.